Chapter 9
Behavior of Tempered Surface Nanocrystalline Structures Obtained by Mechanical-Pulse Treatment

O. Maksymiv, V. Kyryliv, O. Zvirko, and H. Nykyforchyn

9.1 Introduction

Nanocrystalline structures (NCS) and technologies of their production have been a source of great interest to scientists and engineers in recent years because of their unique properties [1]. Obtaining of NCS with high mechanical properties (strength, plasticity, wear resistance, etc.) is particularly important. The technology of mechanical-pulse treatment (MPT) [2, 3] has been recently developed and successfully used for steels to produce surface NCS by severe plastic deformation (SPD) [4], which is generated by energy of high-speed friction. MPT is based on the principle of grinding and can be realized on slightly modified lathes and grinding machines. The physics of MPT consists in a heating of surface layers of treated metal during high-speed friction with the rotational cylindrical tool above the phase transformation temperature (above 850 °C). The peculiarity of the MPT technology is using special fluids, so-called technological media (TM), which are supplied to the friction contact zone and play two roles: (a) enabling structural-phase transformations to occur in the material due to its rapid cooling and (b) saturation of the metal surface layer by chemical elements (carbon, nitrogen, etc.) as a result of thermal and mechanical destruction of TM components within the friction contact zone and intensive mass transfer. Therefore, during MPT two very important processes are realized: (a) metal surface nanostucturization by SPD and (b) metal surface alloying by chemical elements from TM combined with thermal treatment similar to quenching.

Subsequent tempering of NCS is one of the ways to improve its mechanical properties [5]. An important detail for MPT technology is the fact that alloying elements,

O. Maksymiv · V. Kyryliv (✉) · O. Zvirko · H. Nykyforchyn
Karpenko Physico-Mechanical Institute of NAS of Ukraine, Lviv, Ukraine
e-mail: kyryliv@ipm.lviv.ua

O. Fesenko, L. Yatsenko (eds.), *Nanocomposites, Nanostructures, and Their Applications*, Springer Proceedings in Physics 221,
https://doi.org/10.1007/978-3-030-17759-1_9

saturating the metal surface layer, are mainly concentrated at the grain boundaries. Therefore, they suppress the process of recrystallization with temperature increase and facilitate stabilization of NCS [6, 7]. Under the influence of thermal field, force field, and irradiation and during long-term service even at ambient temperatures as well, NCS undergo processes of recrystallization, segregation, homogenization, and relaxation, phase transformation, amorphization, and agglomeration of the nanopores (nanocapillaries) [8]. Differentiation of their impact on mechanical properties of NCS is rather complicated, but almost all of the abovementioned factors significantly influence on properties and service characteristics of NCS. The additional thermal treatment could have the opposite effect on NCS: stabilization of NCS properties [9] on the one hand and their degradation due to partial loss of the initial nanoscale of NCS on the other hand.

The aim of this research was to study the influence of tempering temperature on the structure and mechanical properties of NCS surface layer produced by MPT on 40Kh (0.4C-1Cr) steel.

9.2 Materials and Experimental Methods

MPT was applied to 40Kh steel specimens of two geometries: flat and cylindrical. Flat specimens for X-ray analysis and microhardness measurements were machined from the round bar 25 mm in diameter. The bar was forged to the strip size of 4×32 mm and annealed at the temperature of 860 °C, and after that the specimens with size of $2 \times 20 \times 30$ mm were machined. MPT was applied to both sides of specimens using flat surface grinding machine SPC-20 at the following treatment regimes: tool rotation speed 50 m/s, linear velocity of stage movement 0.0017 m/s, cross-sectional tool advance 0.5 mm on a double-stage movement, and depth of run 0.3 mm (the value characterizes a pressing force of the tool to the treated specimen). Strengthening tool was made of 40Kh steel. Special TM (I-12A industrial oil, GOST 20799-75, with addition of low-molecular-weight polyethylene) was used during MPT for carburizing of the metal surface layer [10].

Cylindrical specimens (rings) 40 mm in diameter and 10 mm thick for wear resistance studies were machined from the round bar and treated by MPT using a slightly modified grinding machine 1 K62 [11] applying the same TM for carburizing at the following regimes: tool rotation speed 50 m/s, rotational speed of treated specimen 0.04 m/s, and depth of run 0.3 mm. Inserts were produced from VCh-60 cast iron (3.3C-2.6Si-0.6Mn-0.3Ni-0.1Cr) in the as-received state. All specimens made of 40Kh steel after MPT were tempered at 200, 300, 400, and 500 °C during 1 h. Wear resistance studies were carried out on friction machine MI-1 M according to ring (specimen)-insert (counter body) scheme [12] in oil medium (I-20A industrial oil, GOST 20799-75) at the load of 2 MPa and sliding velocity of 0.9 m/s. The weight loss ΔG of tested specimens after a certain duration of time (6 h) was considered as the wear parameter. The specimen's weight loss was determined using an analytical balance with a precision of ± 4 mg.

Microhardness H_μ was measured using PMT-3 equipment at the load of 100 g. Phase composition, average grain size, and value of relative stresses in the lattice of the specimen surface layer after strengthening treatment were determined by X-ray analysis using the diffractometer DRON-3 with a CuK_α X-ray source (voltage of 30 kV and intensity of 20 mA), applying a step of 0.05° and exposition of 4 s. The diffractograms were post-processed using the software CSD [13]. The X-ray diffraction patterns were analyzed using the JCPDS-ASTM index [14].

9.3 Results and Discussion

The metallographic studies of the cross section of the flat specimen in depth from the surface revealed the strengthened surface layer as the unetched area (so-called white layer) (Fig. 9.1a). The microhardness of the surface layer of the treated specimen was measured on its cross section (Fig. 9.1b.). It can be visually observed that the size of microhardness indentation imprints in the strengthened layer was smaller than in the matrix material which points to its higher microhardness. The quantitative assessments of H_μ in a depth δ from the surface and from the side of the section (Fig. 9.1a) showed that microhardness varied from maximal value ~ 8.5 GPa on the surface to 2.8 GPa in the matrix material, which was three times less. The thickness of the strengthened layer was ~ 130 μm, and it corresponded with the thickness of the unetched area revealed at the metallographic analysis. Such correspondence points to the responsibility of the unique structure of the strengthened layer for its mechanical property H_μ.

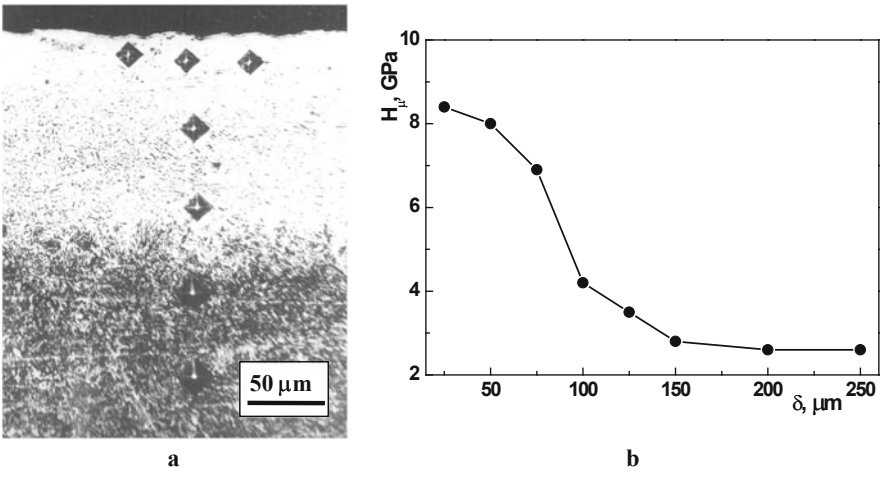

Fig. 9.1 Microstructure (**a**) and microhardness H_μ in depth from surface δ (**b**) of 40Kh steel after MPT

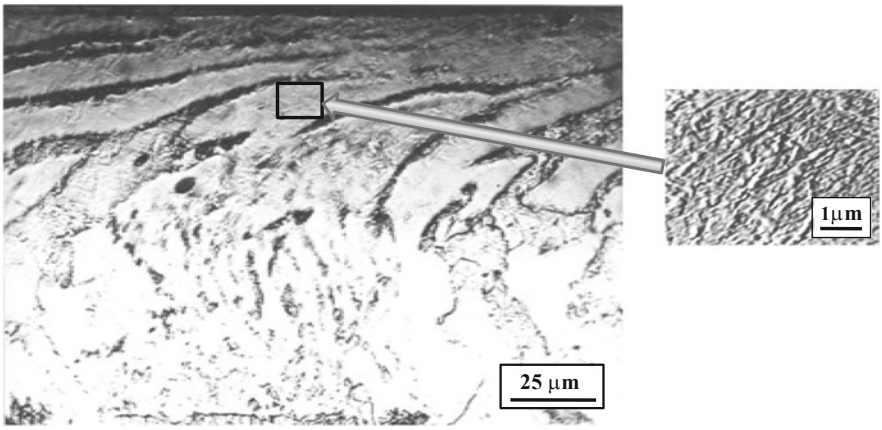

Fig. 9.2 Texture of deformation and fragment of the surface layer of 40Kh steel after MPT

At higher magnifications, the texture of deformation [7] was observed nearly on the surface (Fig. 9.2), which confirmed intense shear deformation necessary for surface nanostructurization during MPT. Dark areas on the surface represent only other crystallographic orientations of theirs compared with light ones, but don't represent an occurrence of another phase. The fragmentation of the structure in the form of unequiaxed stretched areas was observed at even higher magnifications. It allows us to assume that NCS consists of unequiaxed grains as well.

According to X-ray analysis, the steel after MPT had a microstructure, which consisted of pure ferrite α-Fe (Fig. 9.3) with grain size ~ 60 nm. It should be noted that MPT causes heating of surface layers to temperatures above the temperature of phase transformations. Therefore, the appearance of phases, which usually consisted in steel after cooling of austenite, was expected: creation of martensite due to rapid cooling or, at least, formation of cementite, if the cooling rate of the metal was insufficient for martensite transformation. However, martensite and cementite weren't detected on the steel surface after MPT. It could be also assumed that in condition of high-speed heating, there wasn't enough time for formation of an austenite structure, and, accordingly, the initial pearlite structure consisted basically of ferrite and cementite was cooled. Moreover, those phases should be detected by X-ray analysis. In this case, the absence of cementite in the structure of the surface layer was fundamental and could be described in two ways: (a) carbon from cementite dissolved in austenite during heating and martensite didn't form during cooling and (b) cementite decomposed during MPT.

The solubility of carbon in iron lattice at ambient temperatures under equilibrium conditions is negligibly small compared with its content in the steel. So, it can be assumed that all carbon was located at the grain boundaries in atomic state when martensite was absent in the microstructure. Such unconventional state of carbon for ferrite-pearlite steel could be explained by the fact that the total area of grain boundaries in NCS is several orders higher than in the microcrystalline

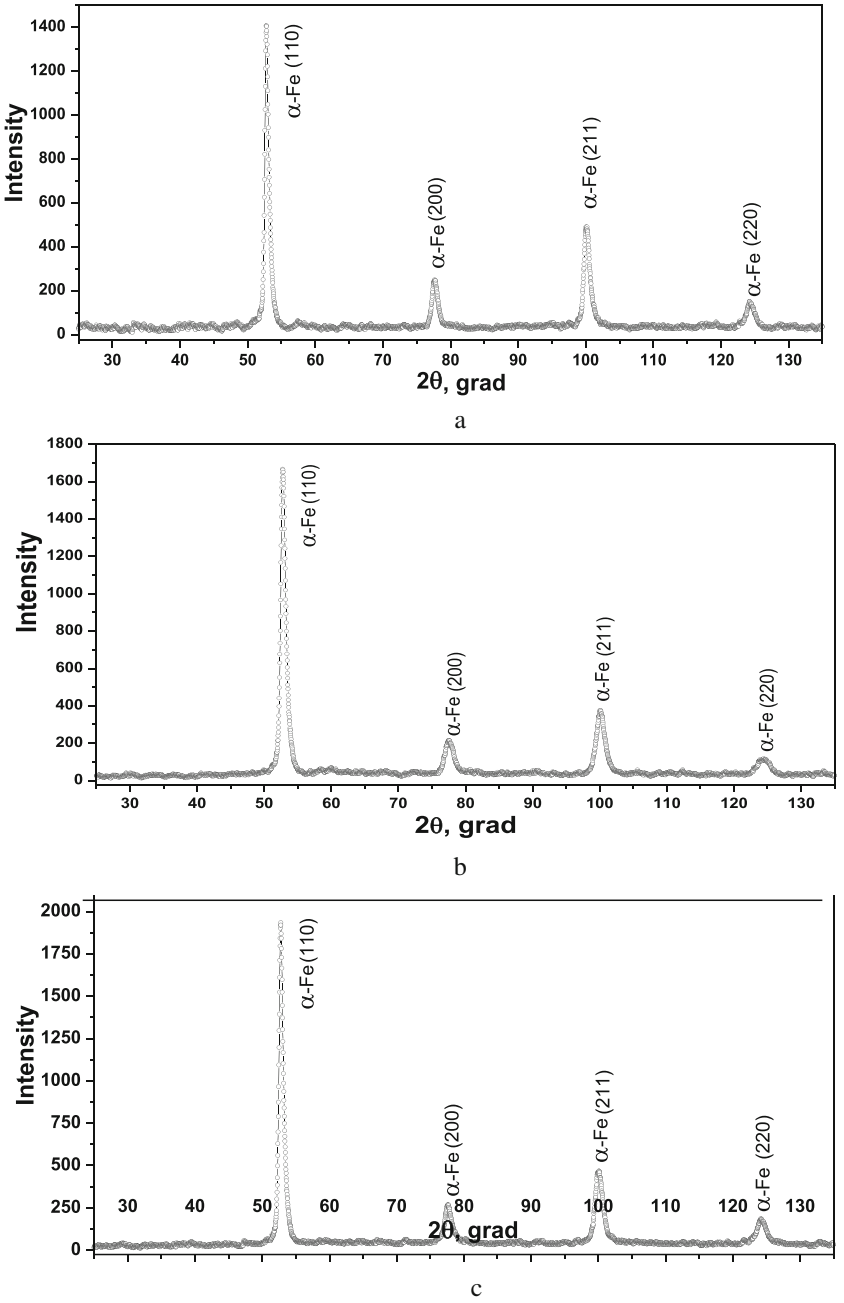

Fig. 9.3 The fragments of diffractograms of surface layers on 40Kh steel after MPT at different tempering temperatures: (**a**) MPT, (**b**) MPT + tempering at 200 °C, (**c**) MPT + tempering at 300 °C, (**d**) MPT + tempering at 400 °C, and (**e**) MPT + tempering at 500 °C

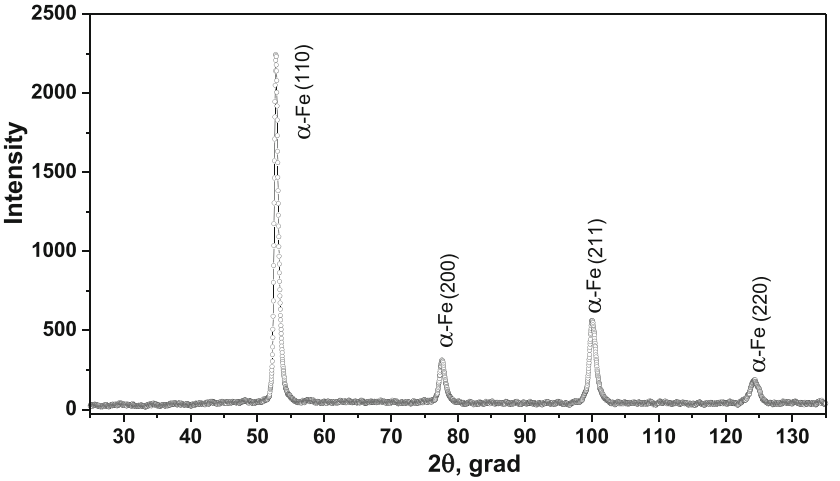

d

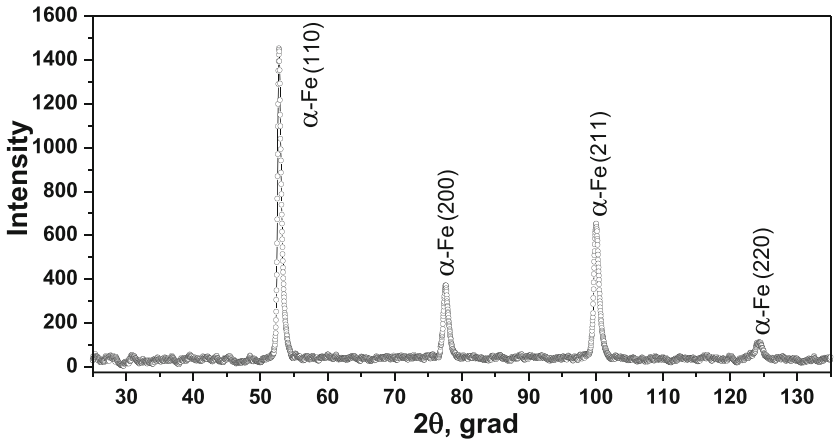

e

Fig. 9.3 (continued)

one. Therefore, the influence of carbon contained in cementite on mechanical properties of microcrystalline steels differs from its influence on the same properties of NCS structures when it is in atomic state at grain boundaries. So, not only extra small grain size but also anomalous carbon state in the steel should be considered at analyzing NCS. It could be expected to detect higher carbon content on the surface NCS layer because of the usage of special TM for carburizing during MPT. Nevertheless, according to carried out analysis, carbon was in atomic state at grain boundaries.

The structural-phase state of steel's NCS layer hadn't been changed after tempering: another component, besides ferrite, wasn't detected (Fig. 9.3b–e). One

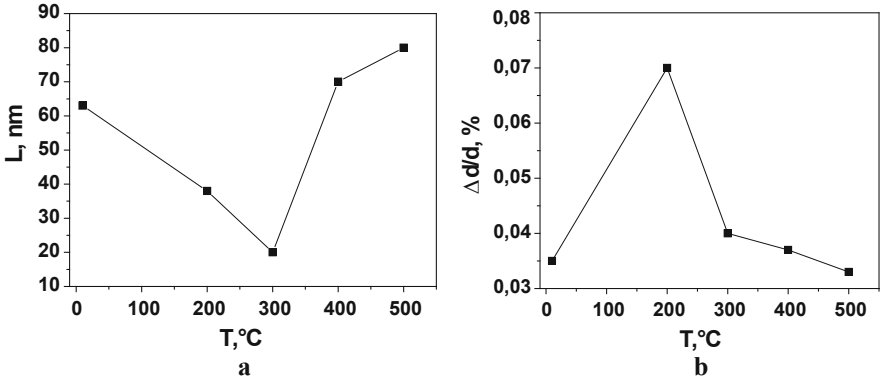

Fig. 9.4 The dependence of the nanocrystalline's grain size L (**a**) and relative stresses of the lattice $\Delta d/d$ (**b**) of surface NCS on different tempering temperatures

Table 9.1 Effect of MPT and subsequent tempering on surface microhardness Hμ of 40Kh steel, GPa

		Tempering at the temperature after MPT			
As-received state	MPT without tempering	200 °C	300 °C	400 °C	500 °C
2.5	8.5	8.4	5.8	5.5	4.4

of the features of MPT treatment is retardation of cementite formation in the studied steel at tempering in such range of tempering temperatures.

Tempering significantly influenced the grain size (Fig. 9.4a), relative stresses in the lattice (Fig. 9.4b), and microhardness of the surface NCS (Table 9.1). Thus, with increase of tempering temperature, the microhardness of the surface layer decreased. However, the microhardness of the surface layer was more than two times higher even after tempering at 500 °C compared with the as-received state. It could be the result of not only retaining of NCS but also enriching of the surface layer by carbon.

The grain size decreased up to about 20 nm with increase in tempering temperature up to 300 °C and then increased. The decreasing of the grain size was unexpected. However, it should be noted that unidirectional shear thermoplastic deformation leads to formation of unequiaxed stretched grains in the surface layer. Then, the fragmentation of unequiaxed grains to more equiaxed grains at the tempering temperature in the range of 200–300 °C was possible, and it resulted in the decrease of grain size L [7]. On the other hand, grain fragmentation needs some level of stresses, which occurred due to tempering. In the studied case, it was shown that the value of relative stresses $\Delta d/d$ in the lattice increased at the tempering temperature of 300 °C compared with the untempered state. This process evidently caused grain fragmentation.

At tempering temperatures above 300 °C, increase of the grain size was accompanied with decreasing stresses in the lattice which indicated the correlation between L and $\Delta d/d$ in all tempering temperature ranges. It should be noted

that the growth of nanograins of the investigated steel occurred at a temperature considerably lower than the temperature of recrystallization. High defectiveness of NCS obtained by SPD creates the field of elastic stresses [15–17]. Complicated structural changes, associated with processes of return, recrystallization, and grain growth, take place during their heating [8]. It should be also noted that heating of NCS to a temperature of 200 °C leads to a sharp reduction of vacancy concentration, and dislocation density is strongly reduced in the temperature range of 200–500 °C [17].

Wear resistance of 40Kh steel with surface NCS depends on the tempering temperature. The highest wear resistance was inherent to the specimens without tempering or after tempering at 200 and 300 °C. In that case, the grains of NCS were the smallest and the microhardness was the highest. At higher tempering temperatures, microhardness and wear resistance of the surface significantly decreased. In general, there was the correlation between H_μ and ΔG. At the same time, it should be emphasized that wear resistance of the surface layer obtained by applying the treatment MPT + tempering at 300 °C (curve 3) was almost the same as at the treatment MPT without tempering (curve 1) or MPT + tempering at 200 °C (curve 2) as it can be seen in Fig. 9.5, but the microhardness H_μ was significantly lower (Table 9.1). On the other hand, MPT + tempering at 300 °C owned the smallest grains of surface NCS (Fig. 9.4a). Hence, it was assumed that the grain refining of NCS was responsible for maintaining of a rather high wear resistance of the surface layer. NCS was characterized by extra low friction coefficient [12, 18, 19], and the positive effect of MPT on wear resistance of the surface layer with reduced microhardness after tempering at 300 °C could be associated with it. Consequently, stable high wear resistance of the surface layer resulted in two confronting factors: decreasing of microhardness and subsequent grain fragmentation. Such unique combinations of properties of NCS, namely, high wear resistance, low friction

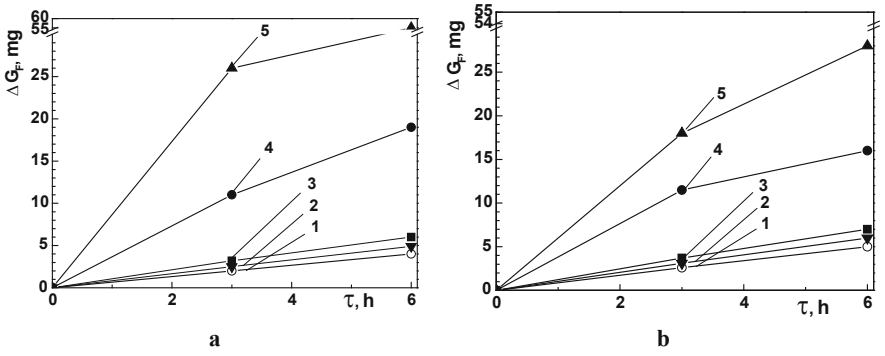

Fig. 9.5 Wear kinetics of rings (**a**) and inserts (**b**) of a pair of 40Kh steel – VCh60 iron tested at a loading of 2 MPa in an oil environment: (1) MPT, (2) MPT + tempering at 200 °C, (3) MPT + tempering at 300 °C, (4) MPT + tempering at 400 °C, and (5) MPT + tempering at 500 °C

coefficient, and low relative stresses, are very important for components working under high-cycle fatigue, corrosion fatigue, and contact loads [20, 21].

9.4 Conclusions

1. Strengthened surface layer obtained by MPT on 40Kh steel formed NCS with defined texture of deformation with unequiaxed grains. It is indirectly confirmed by further refinement of NCS during tempering up to 300 °C.
2. X-ray analysis revealed that the NCS surface layer strengthened by MPT consisted in grains of ferrite only; cementite and martensite were absent. Therefore, all carbon in the NCS surface layer was in atomic state at grain boundaries.
3. Surface NCS without tempering and tempered at temperatures up to 300 °C were characterized by the highest wear resistance. There were two confronting factors that influenced wear resistance: decreasing of microhardness and subsequent grain fragmentation.

References

1. Kurzydlowski KJ (2004) Microstructural refinement and properties of metals processed by severe plastic deformation. Bul Polish Acad Sci Tech Sci 52:301–311
2. Nykyforchyn H, Kyryliv V, Maksymiv O et al (2016) Formation of surface corrosion-resistant nanocrystalline structures on steel. Nanoscale Res Lett 11:51
3. Nykyforchyn H, Lunarska E, Kyryliv V, Maksymiv O (2015) Chapter 32: influence of hydrogen on the mechanical properties of steels with the surface nanostructure. In: Fesenko O, Yatsenko L (eds) Nanoplasmonics, nano-optics, nanocomposites, and surface studies. Springer, Heidelberg/Cham, pp 457–465
4. Umemoto M (2003) Nanocrystallization of steels by severe plastic deformation. Mater Trans 44(10):1900–1911
5. Nykyforchyn H, Kyryliv V, Maksymiv O (2015) Effect of nanostructurisation for structural steels on their wear hydrogen embrittlement resistance. Solid State Phenom 225:65–70
6. Firstov S, Rogul T, Shut O (2018) Hardening in the transition to nanocrystalline state in pure metals and solid solutions (ultimate hardening). Powder Metal Metal Ceram 57:161–174
7. Yurkova A, Belots'ky A, Byakova A (2006) Mechanical behavior of nanostructured layer formed by severe plastic deformation under diffusion flow of nitrogen. Mater Sci Forum 503-504:645–650
8. Andrievski RA (2003) Review Stability of nanostructured materials. J Mater Sci 38:1367–1375
9. Vasiliev MO, Prokopenko GI, Filatova VS (2004) Nanocrystallization of metallic surfaces with using the methods of intense plastic deformation (review). PHYS-USP 5:345–399
10. Kyryliv VI (1999) Surface saturation of steel with carbon during mechanical-pulse treatment. Mater Sci 35:853–858
11. Kalichak TN, Kyryliv VI, Fenchin SV (1989) Mechanopulsed hardening of long components of the hydraulic cylinder rod type. Sov Mater Sci 25:96–99
12. Nykyforchyn H, Kyryliv V, Maksymiv O (2017) Wear resistance of steels with surface nanocrystalline structure generated by mechanical-pulse treatment. Nanoscale Res Lett 12:150

13. Akselrud LG, Gryn' YM, Zavaliy PY et al (1993) Use of the CSD program package for structure determination from data. In: Abstract of the European powder diffraction Conference, Enshede, Netherlands, 1992. Materials Science Forum, vol 41, pp 335–342
14. Powder Diffraction File 1973 (1974) Search manual alphabetical listing and search section of frequency encountered phases. Inorganic, Philadelphia
15. Valiev R, Aleksandrov I (1999) Bulk nanostructured materials from severe plastic deformation. Nanostruct Mater Sci 45:103–189
16. Segal VM (2005) Deformation mode and plastic flow in ultra fine grained material. Mater Sci Eng A 406:205–216
17. Gleiter H (2000) Nanostructured materials: basic concepts and microstructure. Acta Mater 48:1–29
18. Buckleu DH (1981) Surface effects in adhesion, friction, wear, and lubrication. Elsevier, Amsterdam
19. Nykyforchyn H, Kyryliv V, Maksymiv O et al (2018) Wear resistance of the surface nanocrystalline structure under an action of diethylene glycol medium. Applied Nanoscience, Heidelberg, pp 1–6
20. Kyryliv V, Chaikovs'kyi B, Maksymiv O et al (2018) Fatigue and corrosion fatigue of the roll steels with surface nanostructure. J Nano Res 51:92–97
21. Kyryliv V, Chaikovs'kyi B, Maksymiv O et al (2016) Contact fatigue of 20KhN3A steel with surface nanostructure. Mater Sci 51:833–838